Projected changes in synoptic circulations over Europe and their implications for summer precipitation: A CMIP6 perspective

Pedro Herrera-lormendez, Amal John, Hervé Douville, Jörg Matschullat

Received: 23 July 2022 | Revised: 11 January 2023 | Accepted: 24 January 2023 | Published on: 20 February 2023

DOI: 10.1002/joc.8033

RESEARCH ARTICLE

International Journal of Climatology RMetS

Projected changes in synoptic circulations over Europe and their implications for summer precipitation: A CMIP6 perspective

Pedro Herrera-Lormendez[1] | **Amal John**[2] | **Hervé Douville**[2] | **Jörg Matschullat**[1]

[1]Interdisciplinary Environmental Research Centre, TU Bergakademie Freiberg, Freiberg, Germany

[2]Centre National de Recherches Météorologiques, Météo-France/CNRS, Toulouse, France

Correspondence
Pedro Herrera-Lormendez, Interdisciplinary Environmental Research Centre, TU Bergakademie Freiberg, Freiberg, Germany.
Email: pedro.herrera-lormendez@ioez.tu-freiberg.de

Funding information
EU International Training Network (ITN) Climate Advanced Forecasting of sub-seasonal Extremes (CAFE); H2020 Marie Skłodowska-Curie Actions, Grant/Award Number: 813844

Abstract

Projected changes in summer precipitation deficits partly depend on alterations in synoptic circulations. Here, the automated Jenkinson–Collison classification is used to assess the ability of 21 global climate models (GCMs) to capture the frequency of recurring circulation types (CTs) and their implications for European daily precipitation amounts in summer (JJA). The ability of the GCMs to reproduce the observed present-day climate features is evaluated first. Most GCMs capture the observed links between the mean CTs directional flow characteristics and the occurrence of dry days and related dry months. The most robust relationships are found for anticyclonic and easterly CTs which are generally associated with higher-than-average occurrences of dry conditions. Future changes in summer CTs' frequencies are estimated in the high-emission SSP5-8.5 scenario for the sake of a high signal-to-noise ratio. Our results reveal consistent changes, mainly in the zonal CTs. A robust decrease in frequency of the westerlies and an increase in the frequency of easterly CTs favour more continental, dry and warm air masses over central Europe. These dynamical changes are shown to enhance the projected summer drying over central and southern Europe.

KEYWORDS

circulation patterns, climate change, precipitation, weather extremes

1 | INTRODUCTION

Synoptic surface circulations strongly influence the day-to-day weather of any region. The large-scale effects of CT's are dominated by the source of the moving air mass (advective characteristics), the prevailing pressure pattern (high- or low-pressure system) and the time-of-year. Combining these large-scale patterns with local features can lead to weather extremes with devastating effects on society and economic activities. Furthermore, such patterns can influence longer-lasting events (e.g., heatwaves, droughts, floods) if some dry or wet circulation persists over anomalously long periods of time.

Several methodologies were developed to classify such synoptic surface circulations into categories, the circulation types (CTs; not to be confused with weather regimes). Most of these employ atmospheric mean sea-level pressure data (MSLP), or 500 hPa geopotential

heights, to group large-scale configurations (Huth et al., 2008). The Lamb weather types (Lamb, 1972), one of the best-known classifications with its currently updated automated version, can be used to determine the synoptic patterns given a gridded MSLP dataset (Jenkinson & Collison, 1977; Jones et al., 1993). This methodology has been widely used to investigate links between synoptic CTs and variables like temperature and precipitation; most prominently in the UK, where the classification was initially developed (Delaygue et al., 2019; Jones et al., 1993, 2016; Wilby et al., 1997) and later applied to continental Europe and other midlatitude regions (Brands, 2022a; Chen, 2000; Demuzere et al., 2009; Donat et al., 2010; El Kenawy et al., 2014; Lhotka et al., 2020; Lorenzo et al., 2011; Sarricolea Espinoza et al., 2014; Trigo & DaCamara, 2000).

Atmospheric circulation is a major source of uncertainty in climate change projections, including in the midlatitudes (Oudar et al., 2020; Shepherd, 2014). Storylines based on illustrative circulation changes can be used to circumvent this obstacle (Shepherd et al., 2018), but do not lead to a comprehensive probabilistic assessment. Thus, other strategies must be developed to account for circulation changes while assessing changes in regional climate.

The Jenkinson–Collison classification (JCC) often serves as a tool to better understand the influence of CTs on surface climate and, more recently, to investigate changes in seasonal circulation frequency under future climate change conditions. Larger datasets from reanalyses and growing outputs from Global Climate Models (GCMs) in the different generations of the Climate Model Intercomparison Project (CMIP) enabled this approach. However, applications following the original methodology are mathematically limited to areas outside of the equator and the Poles (±5°). Furthermore, its application is recommended to be limited to the latitudes between the ±22.5 and ±80° where the majority of the CTs still occur with reasonable frequency (Fernández-Granja et al., 2023). These limitations are due to the classification's dependency on the marked meridional and zonal pressure gradients that determine the structure and movement of these synoptic surface patterns. Applications from the JCC largely suggest future summer weakening in meridional pressure gradients, directly triggering changes in the average synoptic conditions in Europe—more similar to conditions in the Mediterranean and the south of Europe after the mid-21st century (Herrera-Lormendez et al., 2021). This tendency also suggests seasonal changes in the mean zonal state of synoptic circulations like the westerlies and easterlies as well as cyclones directly influencing regional precipitation changes, for example, over the British Isles (Burt & Ferranti, 2012).

Some of these findings advocate for more frequent rainy westerly circulations over northern Europe in winter and a corresponding decrease in easterlies and cyclonic circulations over the Mediterranean (Cahynová & Huth, 2016; Demuzere et al., 2009; Hoy et al., 2014; Stryhal & Huth, 2019b). On the other hand, summers show weakening westerly inflow with a corresponding increase in the frequency of some easterly advection over western and central Europe (Otero et al., 2018). Such projected increase of dry CTs to the detriment of rain-rich synoptic circulations supports current IPCC projections for wetter winters over northern Europe and drier conditions southward, as well as a generalized decrease in summer precipitation across Europe and rainier conditions towards the northernmost part of the region (Douville et al., 2021; Santos et al., 2016).

Much previous work focuses on the winter season, given better discernibility between the CTs due to stronger pressure gradients at that time of year, and the clearer signal these patterns have on surface climate variables. Nevertheless, summer will become a challenge for southern Europe, where precipitation amounts are expected to significantly decrease (Douville et al., 2021). Under a global warming scenario, where greenhouse gases continue to rise, the poleward shift of the Hadley cell edge will proceed (Grise & Davis, 2020). Ramifications of these changes will influence, for example, heat waves becoming more frequent, with higher mean duration, extent, and intensity (Schoetter et al., 2015) and more severe droughts with longer-lasting effects (Lhotka et al., 2020; Schwarzak et al., 2015). Nonetheless, some of the consequent changes in MSLP and associated circulation might directly strengthen or mitigate the projected precipitation changes over Europe (Belleflamme et al., 2015), as other large-scale phenomena, local thermodynamic factors, and the dynamics within the changing CTs themselves might dominate over these alterations.

The objective of our study is to use a well-known and fixed classification of summer synoptic CTs to study changes in their relative frequencies and their influence on summer daily precipitation amounts over Europe. We investigate (i) the links between European synoptic circulations and dry days; evaluate (ii) how well GCMs reproduce the summer features of these patterns when compared to the ERA5 and E-OBS datasets; study (iii) the influence of dry circulations on the subseasonal time scale during anomalously dry months; explore the (iv) likely future frequency changes within the CTs towards the end of the current century and their impact on projected rainfall changes; and apply (v) a linear decomposition of frequency and precipitation changes to better understand the contribution of CT frequency changes to projected precipitation anomalies.

2 | DATA AND METHODS

2.1 | Gridded Jenkinson–Collison classification

We follow the methodology proposed by Otero et al. (2018) by adapting the JCC with a moving central grid point to compute the corresponding gridded CTs over the European domain (15°W–30°E and 35°–70°N). This adapted version allows us to classify time-step synoptic configurations at each grid cell to later assess the influence of the dominant CTs on any atmospheric variable during the chosen time frame (Figure 1). This adapted version has been developed and published as a Python module named "jcclass" (Herrera-Lormendez, 2022). Its documentation provides further insight to the method, its usage and reproducibility (see Data availability statement section). The full classification initially considers 27 different synoptic circulations based on dominant MSLP features (cyclones and anticyclones) and their wind flow directions plus a "Low Flow" (LF) type. This last CT is characterized by days with very weak pressure gradients, making it difficult to relate them to any dominant advection (Otero et al., 2018 for more information on the method). Here, for the sake of simplicity, we aggregate some neighbouring CTs based on their flow direction and only consider 11 types: the Anticyclonic (A) and Cyclonic (C) centre pressure systems, the corresponding eight prevailing directions of advection (NE, E, SE, S, etc.) and the remaining LF type. Yet, our method could be easily applied to the original JCC and would lead to similar conclusions.

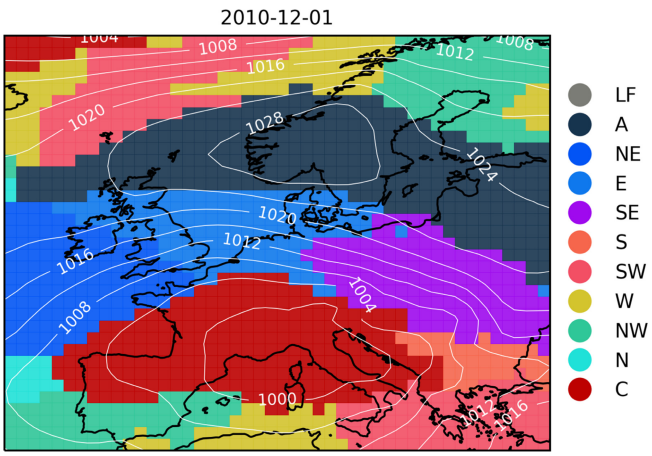

FIGURE 1 Gridded 11 synoptic circulations (CTs) and daily mean sea-level pressure isobars (MSLP; 1° × 1° resolution) on a given day (here 1 December 2010) over the study domain (15.5°W–30.5°E and 35.5°–70.5°N). Computed with the jcclass python module (Herrera-Lormendez, 2022) [Colour figure can be viewed at wileyonlinelibrary.com]

2.2 | Influence of CTs on dry days and months

Daily MSLP from ERA5 reanalysis (Hersbach et al., 2020) was employed to calculate daily synoptic circulations. Here, we combine the preliminary ERA5 version (pre-1979) with the already available ERA5 dataset (1979 onwards). Daily rainfall totals from the E-OBS gridded dataset (Cornes et al., 2018) were used to investigate the CTs' influence on daily summer (JJA) precipitation patterns. ERA5 (MSLP) and the combined ERA5/E-OBS (MSLP/precipitation) were used as reference datasets. A subset of 21 GCMS from the sixth phase of the Coupled Model Intercomparison Project (CMIP6), based on the historical experiment (1951–2000) and the SSP5-8.5 scenario (2051–2100), were included in our analyses (Table S1, Supporting Information for a GCMs list). All datasets were interpolated onto a 1° × 1° common horizontal grid using bilinear and conservative methods to facilitate the model evaluation and intercomparison.

To investigate the CTs' influence on dry days, we compute the conditional probability of a dry day (CPDD) for each circulation pattern by accounting for all summer days with total precipitation below one millimetre on each grid point of the European domain, divided by the total summer relative frequency corresponding to the individual CTs.

To further explore their influence on dry months, we compute the Pearson 1-month standardized precipitation index (SPI), given its advantage of using only precipitation as the input parameter for its computation. The SPI calculation is based on the long-term precipitation record from the 1951–2000 period. This long-term record is fitted to a probability distribution, which is then transformed into a normal distribution so that the mean SPI for a desired location and period is zero. The resulting SPI values serve as an indicator for higher and less precipitation than the median when values are positive and negative, respectively. Its application can be also used to define drought events at times when the SPI continuously remains negative reaching values of −1.0 or less (Edwards & McKee, 1997; McKee et al., 1993). We use monthly aggregated rainfall from the different datasets, resulting in a monthly-SPI gridded timeseries that represents the degree of dryness (SPI < −1) and wetness (SPI >1) over a chosen period. We employ 1-month SPI as it better reflects short-term dry conditions, which can affect, for example, soil moisture and crop stress during summer (Svoboda et al., 2012). The SPI index was calculated using Adams's Climate Indices python package (Adams, 2017). Only dry and very dry months were analysed, meaning that we only keep those months with SPI values below −1. The gridded monthly frequency

anomalies of each CT, taking place during the given dry months, were computed to derive the monthly anomalous occurrences of these patterns during the summer season.

2.3 | Attribution decomposition of future precipitation changes

Our main objective is to assess how changes in the CTs' frequency can contribute to an overall summer drying over Europe (Douville et al., 2021) and how model-dependent such a contribution can be. We tackle this by deriving future changes in the summer frequencies of the synoptic patterns, based on the difference between the late 21st century (2051–2100) and the historical reference period (1951–2000). We compute the spatial changes throughout the individual models and display the resulting multi-model ensemble mean (MMEM) and the corresponding multimodel agreement.

To investigate the attribution, corresponding to the projected changes in CTs' frequencies on precipitation over Europe, we use the same linear decomposition equation as in Cattiaux et al. (2013) but using fixed rather than time-evolving circulation types. So doing, we can easily decompose future climatological changes in a variable X (here precipitation) as follows:

$$\Delta^{F-P} = \overline{X}^{F} - \overline{X}^{P} = \underbrace{\sum\nolimits_{k} \Delta f_{\kappa} \cdot x_{k}^{P}}_{\text{BC}} + \underbrace{\sum_{k} f_{k}^{P} \cdot \Delta x_{k}}_{\text{WC}} + \underbrace{\sum_{k} \Delta f_{k} \cdot \Delta x_{k}}_{\text{RES}}, \tag{1}$$

where $f_k = \frac{N_k}{N}$ is the frequency of occurrence of the kth circulation type and x_k is the precipitation conditional mean to regime k, defined by $x_k = \frac{1}{N_k} \sum_{i \in \Omega_k} X_{ik}$ with Ω_k being the total ensemble of the N_k days classified in the kth CT.

Equation (1) describes how changes in the frequency of the synoptic circulations contribute to changes in $\overline{\boldsymbol{X}}$. This can be estimated considering the difference between two time periods, for example, future (F) and present (P) climate. The first term is "Between-Class (BC)," representing the part of the total difference of precipitation due to frequency changes in the circulation types, that is, an observed drying might be due to more frequent appearance of "dry" atmospheric circulations. The second term is "Within-Class (WC)," referring to the contribution of differences within the CTS which can be related to both thermodynamic and mesoscale dynamic processes, while the third one, "Residual (RES)," is defined as a mixing term. Here, the breakdown of total changes is applied at each grid cell over the chosen European domain, allowing us to showcase the spatial distribution of the proposed decomposition.

3 | RESULTS

3.1 | Spatial distribution of CT frequency and influence on dry days

Synoptic circulations owe their existence to the surface pressure gradients that shape the low-level horizontal winds and influence local weather through temperature and humidity advection. The probability of a dry day (PDD) in Figure 2a depicts the summer probability of occurrence of days with precipitation <1 mm over Europe. Overall, the incidence of precipitation strongly varies meridionally, and it is influenced by mountain ranges (Alps and Carpathian Mountains) and by moisture transport from the Atlantic (British Isles and western Scandinavia). In contrast, regions were most of the summer days do not record rainfall are those around the Mediterranean due the northward extension of stable subtropical conditions.

By isolating the spatial summer occurrence of a given CT, we can derive its seasonal relative frequency (RF) as well as its influence on rainfall. Here, we have selected one CT (the westerly type) to illustrate this method. Figure 2b shows the summer spatial RF of the westerly circulation (W) during the 1951–2000 reference period derived from ERA5 reanalysis. The westerlies draw a well-defined belt of influence that extends from the west of the British Isles to northern central Europe. The westerlies appear southwards of cyclonic centres and northward of the high-pressure systems. Their maritime origin helps regulate temperatures over western Europe and are an important source of humidity advection for this part of the continent. Their strong influence on the daily summer precipitation can be seen in Figure 2c as the CPDD. This metric is derived by combining the CTs obtained from ERA5 MSLP and the daily rainfall data from the E-OBS dataset. The occurrence of the W type is very likely to cause precipitation (blue colours) over regions like western Scandinavia, the Alps and western British Isles, and in less proportion over the rest of western continental Europe where they are frequent, because of direct maritime air masses transport from the Atlantic Ocean.

The Supporting Information yields additional figures of RF and CPDD (S1a and S1b). First, we briefly discuss the RF′ spatial characteristics of the other CTs. Overall, the anticyclonic circulation is the most frequent pattern (20%), generally with an evenly distributed RF over the continent. Its frequency predominates over the Atlantic

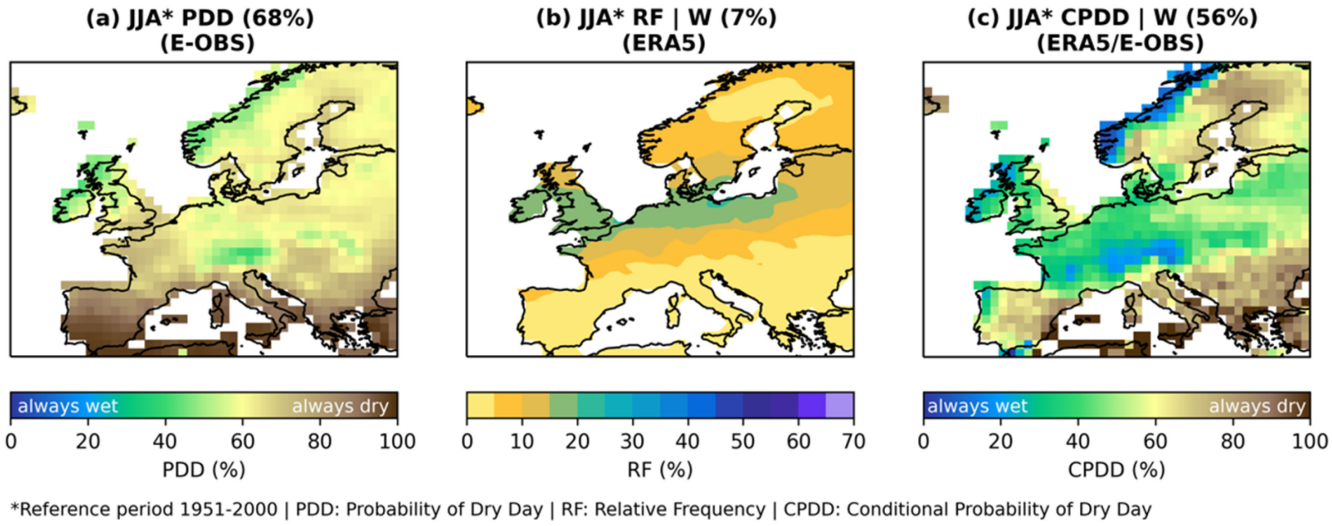

FIGURE 2 Summer (JJA) conditions during the 1951–2000 reference period. (a) Probability of dry days (PDD) based on E-OBS dataset. (b) Relative frequencies (RF) of westerly circulation type (W) derived from ERA5. (c) Conditional probability of dry days (CPDD) of westerly circulation type (W) based on ERA5 and E-OBS. "(%)" Continental pan-European spatial mean value of PDD, RF and CPDD, respectively. Complementary plots found in Figure S1 [Colour figure can be viewed at wileyonlinelibrary.com]

Ocean and extends towards continental Europe, given the extension of the Atlantic High that dominates summer months over the Azores. The second most frequent CT is the LF (19%), characterized by weak pressure gradients. This CT is more often observed in summer and is linked to a dominant ridge configuration (extension of a high-pressure system), distinct from the anticyclonic CT. The LF pattern dominates over half of the summer days in southern Europe, as expected from the northward extension of subtropical weak meridional pressure gradients during JJA over this region. Contrastingly, the cyclonic, the third most dominant pattern (12%), prevails over the northern latitudes as these centres of low-pressure systems move incessantly from west to east. The fourth and fifth most common types are the NE (9%) and N (8%) types. Their occurrence is higher around the Mediterranean and corresponds mainly to the eastward flanks of the anticyclonic circulations. A similar pattern to the one observed in the W can be derived in the NW (7%) type with an overall frequency constrained around the 55° latitude belt. The eighth most common pattern during summer is the easterly (E). Its occurrence, for example, over central Europe, is often associated with a dominant anticyclone over northern Europe; at times linked with heatwave events, dry days, and the advection of hot air from the inner continent (Herrera-Lormendez et al., 2021). The remaining circulation types (SW, S and SE) account for the remaining 12% of the variability. However, their occurrence is limited to very determined areas mainly covering northern Europe.

Figure S1b shows the probability of a dry day during the occurrence of the remaining circulation types (CPDD). It confirms the well-known fact that anticyclones are responsible for dominant subsidence conditions and clear skies without rainfall. On average, 91% of the days under their occurrence do not favour rainfall. Exceptions to this rule appear in localized, orography-dominated areas such as the Alps, a possible result of mountain-favoured isolated convective storms. The LF type does not show a marked influence on precipitation over most of continental Europe. About half of the time, this pattern is linked with rainfall, albeit mainly over inland regions. We attribute this behaviour to dominant calm summer days in which warming over land can trigger small-scale convection events (summer storms) depending on moisture availability and previous weather conditions. The opposite becomes clear for the cyclonic type, where precipitation generally occurs when a cyclone moves through a region. Mediterranean coastal areas make for an exception, where this circulation takes place on less than 15% of the summer days. The NE and N types mainly influence rain events over the coast of Norway and over the European mountain ranges due to moisture advection from the North Sea. Circulations with a dominant westerly component (NW, W and SW) are very likely to be accompanied by rainfall as they bring humid air from the Atlantic and Mediterranean. Adversely, the easterly component CTs with inland origin (E and NE) mainly favours dry conditions over the continent. The western part of Europe experiences the E and NE patterns as dry; barely responsible for rainy events as

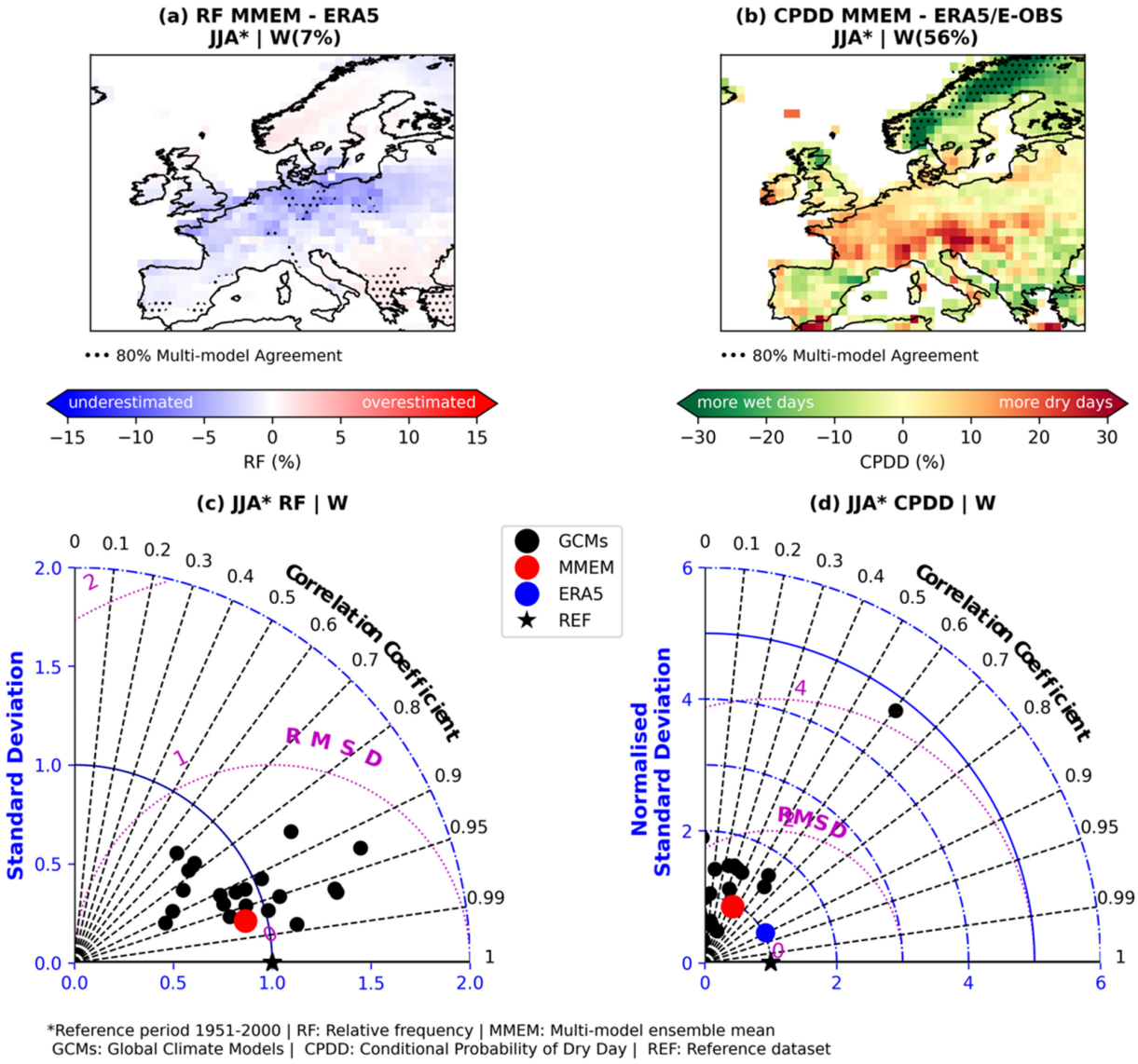

FIGURE 3 Evaluation of GCMs' performance of the westerly circulation type (W) during summer (JJA). Top row shows the spatial biases of (a) Relative frequencies (RF) from the MMEM minus ERA5; (b) conditional probabilities of dry days (CPDD) from the MMEM minus ERA5/E-OBS. "(%)" in (a) and (b): continental pan-European spatial mean value of RF (ERA5) and CPDD (ERA5/E-OBS), respectively. Stippling in (a, b) indicates a multimodel sign agreement of the biases of at least 80% of GCMs. Complementary plots found in Figures S2 and S4. The bottom row displays Taylor diagrams comparing the performance of the individual GCMs and the MMEM for (c) RF compared to ERA5 and (d) CPDD compared to ERA5/E-OBS. Extra dot in (d) shows the performance of ERA5 when using both MSLP and rainfall to derive the spatial CPDD [Colour figure can be viewed at wileyonlinelibrary.com]

they bring drier and warmer air from central Europe. However, in some places like southeastern Europe, they can produce precipitation given the influence of the Mediterranean and the Black Sea.

It is also important to point out that when employing the ERA5 precipitation data to evaluate the CPDD, ERA5 dataset tends to consistently capture more rainy days (daily rainfall above 1 mm) as compared to the E-OBS gridded dataset (Figure S7). This agrees with previous findings pointing out that ERA5 tends to overestimate mean precipitation related to too many wet days over Europe as compared to E-OBS (Bandhauer et al., 2022).

3.2 | Model evaluation

Our analysis is based on the latest generation of GCMs which have contributed to CMIP6 (Eyring et al., 2016). This new generation of GCMs showed an improved ability to reproduce the JCC-derived synoptic CTs compared

to the former CMIP5 GCMs (Fernandez-Granja et al., 2021). Yet, models still show contrasted skills in reproducing the summer mean frequency of the classified CTs over Europe. To compare the RFs obtained from ERA5 reanalysis against those derived from the climate models, we compute the MMEM of the 21 available GCMs over the reference period 1951–2000. For visualization, we only display the results regarding the previously analysed W circulation. Figure 3a shows the spatial RF biases for this CT. This was derived by computing the difference of the summer RF in the MMEM minus ERA5 during the 1951–2000 reference period. The mean pan-European spatial RF values are given in brackets for reference. By method design, GCMs are generally able to reproduce the spatial features of the various circulations. However, GCMs tend to underestimate the frequency of the W type along their area of influence, extending from the UK and eastwards onto the continent. Such discrepancies have been documented in previous evaluations hinting to model biases due to erroneous simulation in Mediterranean circulation and North Atlantic sector (Huguenin et al., 2020; Stryhal & Huth, 2019a). However, a multimodel agreement of at least 80% of the models in the sign of the biases is not reached over most of the area where these biases appear, showing large model uncertainty. These biases in RF are individually assessed in the climate models through Taylor diagrams (Figure 3c). The spatial correlation of the RF of the W type is high in most of the individual GCMs (black dots) and in the MMEM (red dot). Nevertheless, the normalized standard deviation (SD) reveals the important spread that prevails between the models. The ensemble-mean spatial biases agree with the ones found in the previous evaluation of the fifth generation of CMIP (CMIP5; Otero et al., 2018).

Remaining spatial biases and Taylor diagrams of the other CTs are displayed in Figure S2a,b. These show that the summer underestimation of the RF in the W type replicates to the other westerly component types like NW and SW. The biases in the anticyclones are less homogenous but are generally underestimated throughout the western parts of Scandinavia, UK, Iberian Peninsula and along the mountain ranges. They are overestimated over the central and eastern part of the Mediterranean as well as central Europe. These spatial biases are reflected in the spatial correlation coefficient (CC) values in the Taylor diagram, resulting in some of the lowest values in the individual GCMs. Furthermore, their higher SDs reflect the more significant intermodel spread. The LF pattern is generally underestimated over the Mediterranean region, but with very good spatial CC values in most climate models. Some of the circulations with the overall lowest CCs are those of northerly and easterly component (N, NE, E types) which tend to be overestimated over the continent. In most cases the worst metrics in the SD and CC are consistently observed in the INM-CM4-8 and INM-CM5-0 climate models. Yet, models with some of the best scores vary regionally from one circulation to another. Overall, models like the MPI-ESM1-2, EC-Earth3 and MIROC6 stand out as some of the ones with better performance at reproducing the RF patterns during summer (Figure S3).

We also evaluate the models' ability to capture the probability of dry days during the occurrence of the different CTs. Figure 3b shows the MMEM biases relative to the combined ERA5/E-OBS dataset of the summer CPDD (precipitation <1 mm) related to the W circulation. Stippled areas show at least an 80% multimodel agreement in the sign of the biases. Values in brackets state the spatial mean value of the CPDD, based on the reference dataset ERA5/E-OBS. The spatial biases found under the influence of the W type are stronger over Scandinavia and Scotland. Here, at least 80% of the GCMs tend to capture more wet days (precipitation >1 mm) as compared to the reference dataset. However, the opposite is observed over the Alps and France, where more dry days occur. This poor agreement between the GCMs and the reference dataset in properly capturing dry days becomes more evident when looking at each individual model's performance in the Taylor diagram in Figure 3d. In most cases, GCMs show poorer spatial correlation values (below 0.6). Some models even result in negative CC values (Figure S5b). In comparison, we can see the resulting performance of ERA5 (blue dot) if this dataset were to be used to compute the CPDD by employing both its MSLP and precipitation. As expected, ERA5 would outperform all individual climate models in capturing the distribution of the dry days.

The biases of the other 10 CTs are shown in Figure S4 and are described next. Overall, we find that GCMs tend to display more dry days over land areas (except Scandinavia). In contrast, more rainy days are captured over the northern parts of Europe and especially over Scandinavia during the influence of most circulations; especially those having strong influence on wet days. Some of these differences are more evident within the C type, where models generally identify more dry days southwards of the continent, whereas more rainy days generally occur in Scandinavia and the northern part of Britain. However, despite what might look like a strong signal in the south, the multimodel agreement remains confined to only some areas. These regions, where some of the models capture more dry days, coincide with those where these CT frequencies are generally slightly overestimated by the ensemble members. Anticyclones, however, show the smallest differences in capturing the lack of precipitation associated with the days dominated by these high-

pressure systems. The Taylor diagrams (Figure 3b) show how the MMEM and most of the models fail to properly capture the spatial distribution of these patterns (correlation coefficients below 0.7). Overall, CC values are smaller in comparison to Figure 2b, due to higher spatial precipitation variability. The disagreement in the individual models is more visible in the W and C types with the lower SDs and CCs. Various GCMs continue to differ significantly in their ability to accurately represent westerly patterns and their distribution of precipitation. These characteristics are prevalent in the westerly-related types (NW, W and SW) shown in Figure S4.

3.3 | Links with dry months

The day-to-day influence of CTs can affect onset, duration and strength of long-lasting events like dry spells and heatwaves. The individual influence of each CT on longer time scales can vary significantly from one pattern to another. It has been shown previously that the increased monthly frequency of some anticyclonic patterns can directly influence regional droughts (Phillips & McGregor, 1998; Richardson et al., 2018). Therefore, it may be important to assess the long-term behaviour of these CTs in a warmer climate, as any significant change in their frequency may favour the occurrence of some extreme events (Neal et al., 2016).

To address this, we investigated the fingerprint of the synoptic circulations on monthly precipitation deficits by computing the monthly SPIs and isolating the dry months with SPI < -1. Then, we compute the gridded monthly anomalies in CT frequency conditional on dry months. Figure 4a displays the present-day (1951–2000) monthly frequency anomalies derived from the combined ERA5 reanalysis (derived CTs from MSLP fields) and the E-OBS precipitation data (SPI values). Not surprisingly, one of the strongest and more homogenous increases in frequency arises in the A type. Its positive frequency anomalies are evenly distributed over the continent, albeit with a more evident influence over northern Europe and the UK. On average, high-pressure centres (anticyclones) increase their frequency by 29% during dry months. The appearance of anticyclones over northern Europe is reflected in the increment of the E, NE and SE types over western and central Europe. The influence of the E and NE types is more marked along the Atlantic coast of Europe and over the British Islands, whereas the SE pattern increases its frequency over central Europe during these months, though with a more scattered spatial occurrence. This anomalous occurrence of easterly advection can occur during Scandinavian blocking events that are often responsible for longer-lasting heatwaves and dry conditions as they favour the transport of dry, warm continental air from mainland Europe (Ionita et al., 2020; Kautz et al., 2022; Pfahl, 2014). On the contrary, and as expected, the cyclonic and westerly-like circulations (NW, W, SW), responsible for many rainy days over Europe, considerably decrease in frequency during dry months. The appearance of cyclonic centres is almost halved (−47%) during dry months. This behaviour happens as the establishment of anticyclones and easterlies block the influence of humid westerly advection over the continent (Pfahl, 2014). The remaining CTs show weaker signals during these dry events. The LF type, for example, plays a negligible role in the appearance of dry months as, generally, they do not show significant positive or negative anomalies in their occurrence. This comes as no surprise, since the LF type favours mainly isolated precipitation events during summer.

For comparison, Figure 4b shows the corresponding monthly frequency anomalies corresponding to the MMEM estimated from the 21 CMIP6 GCMs during the reference period. Stippling highlights the areas where at least 80% of the models agree with the sign of the ensemble mean anomalies. Overall, despite the noisier ERA5 patterns that arise from comparing a single reanalysis to a multimodel dataset, the models do capture the sign and the predominant spatial distribution of the observed monthly frequency anomalies associated to dry months. However, the multimodel agreement never reaches 80% in the case of LF type given its negligible influence on the apparition of dry months also reflected in the GCMs. This lack of multimodel agreement is also observed for the S and SE types despite the later showing an overall European influence on dry months. The highest multimodel spatial agreement appears for cyclones and anticyclones given their stronger influence on favouring precipitation and dry days respectively.

3.4 | Future changes and contribution of CT frequencies

The CMIP6 GCMs have been shown to work reasonably well at reproducing the spatial characteristics of the RF of most synoptic CTs, albeit still with important biases in some individual models for anticyclones and easterly types. When evaluating the precipitation fingerprint associated with the different CTs, the models generally overestimate the number of dry days over continental Europe (except Scandinavia) during the occurrence of rainy types like the cyclonic and westerlies. A general tendency prevails in capturing more rainy days over Scandinavia when compared to the reference dataset. Bearing in mind such limitations, our next step is to analyse changes in

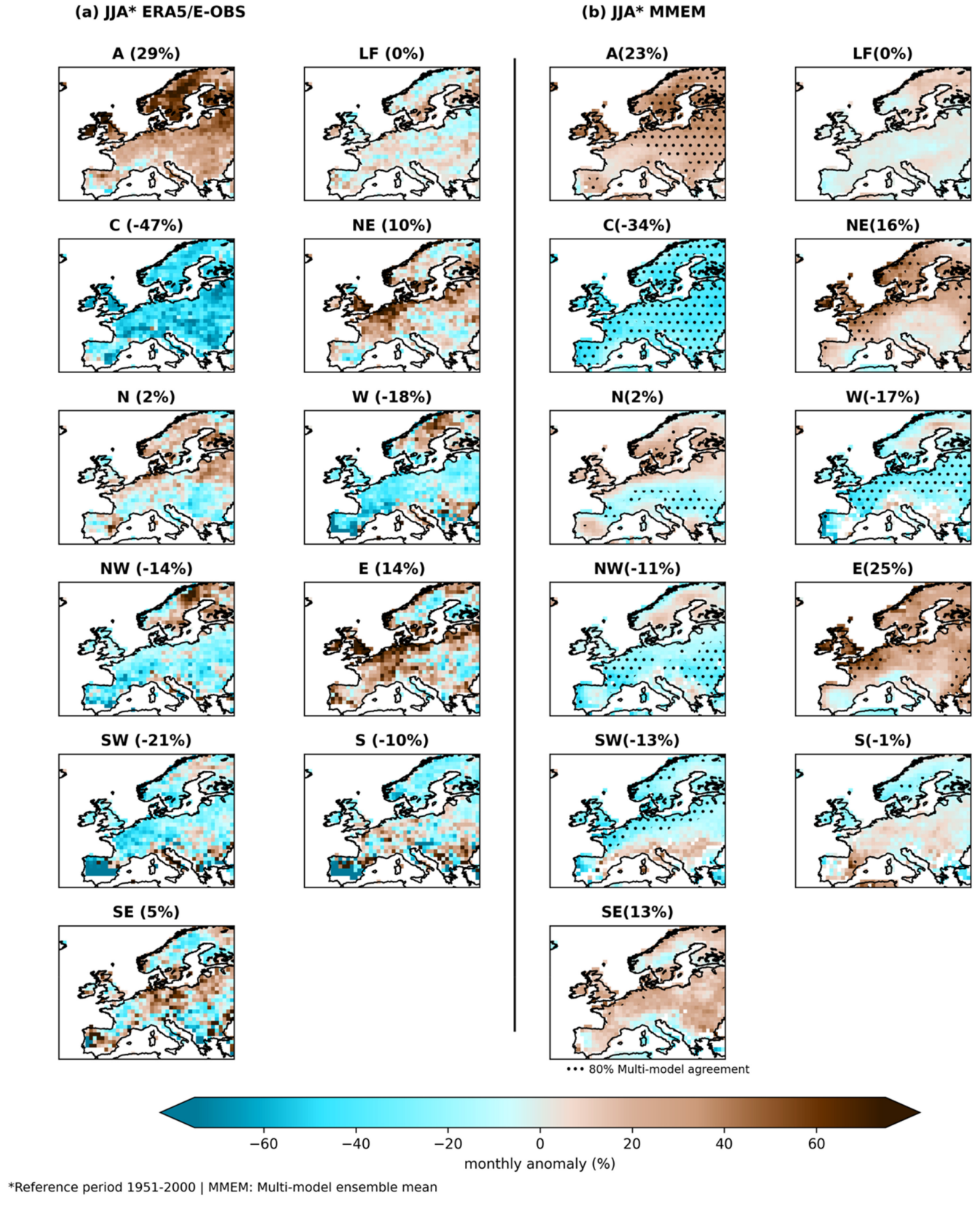

FIGURE 4 Monthly anomalies in circulation type (CT) frequencies (1951–2000) conditional on SPI < −1 in (a) ERA5/E-OBS and (b) CMIP6 multimodel ensemble mean (MMEM) during summer (JJA). Stippling in (b) indicates a multimodel sign agreement of at least 80% of GCMs. "(%)": Continental pan-European spatial mean value of the monthly anomalies [Colour figure can be viewed at wileyonlinelibrary.com]

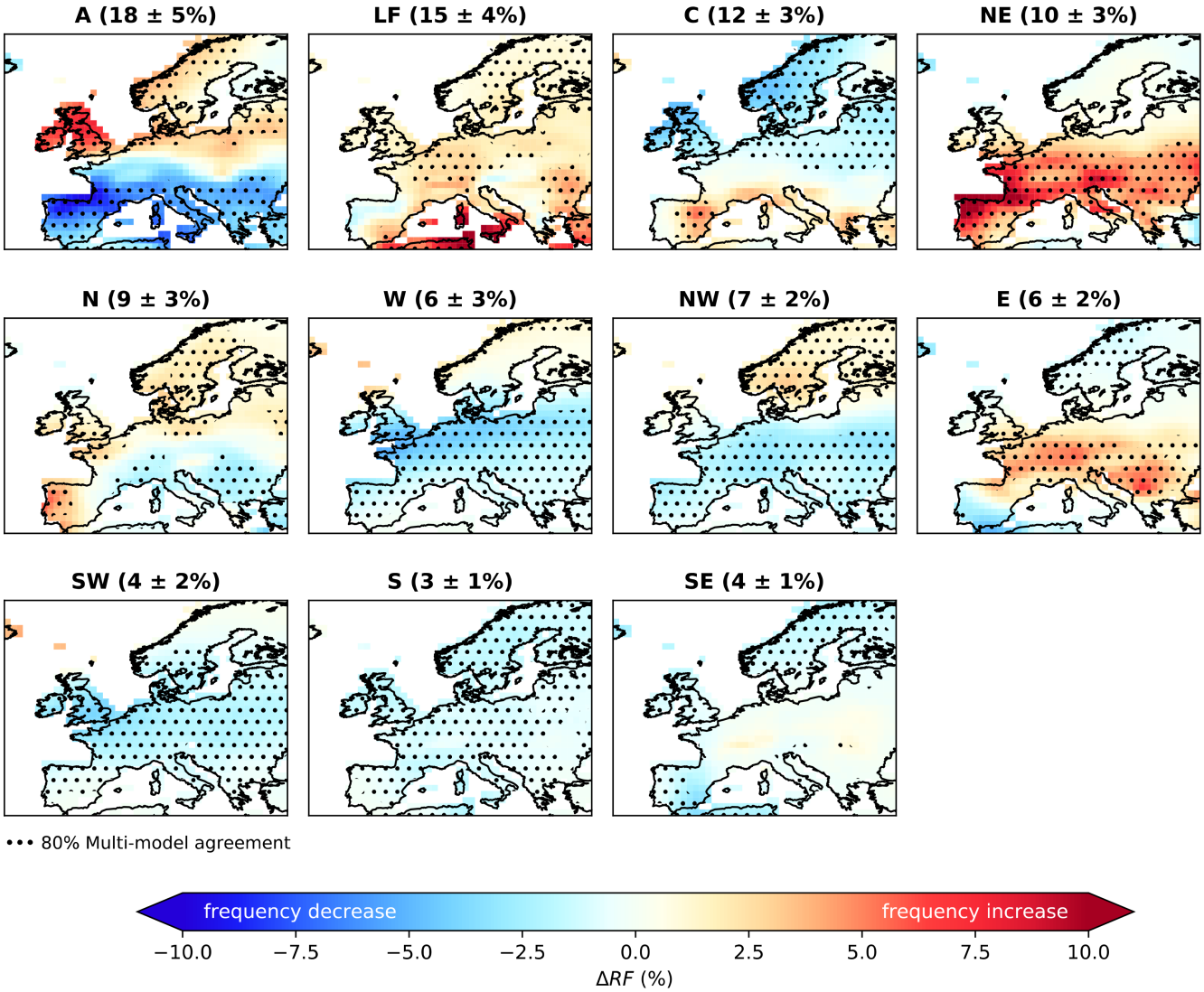

FIGURE 5 Future changes in summer (JJA) relative frequencies (RF) over continental Europe. Changes are computed based on the mult-imodel ensemble mean (MMEM) future (2051–2100) minus the MMEM reference (1951–2000) periods of RF. Stippling indicates 80% multimodel sign agreement. "(%)": Continental pan-European spatial MMEM value of RF ± one standard deviation during the 1951–2000 reference period [Colour figure can be viewed at wileyonlinelibrary.com]

CT frequencies in a warmer climate and their implication for precipitation. Therefore, we estimate the anomalies in summer RF and precipitation conditioned to each CT between 2051–2100 in the SSP5-8.5 scenario and 1951–2000 in the historical simulation. For the sake of simplicity and equal treatment of each model, we only employ the first member (r1) of a subset of 21 GCMs from CMIP6 (Table S1 for a list of the individual GCMs).

Figure 5 depicts these projected changes in RF computed from the MMEM, with the hatched areas showing an 80% multimodel sign agreement. The values in brackets serve as a reference showing the pan-European spatial mean value of RF derived from the MMEM ± one standard deviation resulting from the intermodel spread. The order of the CTs follows the most to least frequent type resulting from the ERA5 reference dataset. Anticyclones and cyclones largely depict symmetric responses. The North Atlantic storm track within the domain shows consistent decrease in the frequency of cyclones. This agrees with the projected, near 5% decrease in the number of extratropical cyclones systems by the end of the 21st century (Priestley & Catto, 2022). Contrastingly, influence of anticyclones is expected to increase northwards the +50° latitude belt extending from the British Isles to Scandinavia. As a response, the midlatitude summer cyclones that generally move eastwards will likely lose their influence over these regions. An apparent increase of cyclones as a response to a weaker influence

of anticyclonic centres appears over the Mediterranean. Cyclone occurrences over the Mediterranean were found to have a close connection with localized extreme precipitation events (Mastrantonas et al., 2022). However, areas with an 80% multimodel agreement are limited to the western part of Spain. Furthermore, this projected increase in cyclonic conditions over the Mediterranean is strongly influenced by the previously analysed present-day biases (Figure S2). Some of the worst performing GCMs at over-representing this CT over western and southern Europe (INM-CM4-8, INM-CM5-0 and KACE-1-0-G) contribute to a strong positive intermodel correlation with the projected circulation changes for unclear reasons that remains to be explored (Figures S8 and S9).

The dominant summer LF type exhibits a generalized northwards increase in frequency across most of the domain. This expansion translates into more days with weather more akin to that of southern Europe. That agrees with a projected weakening of near-surface wind speed over land under anticipated high greenhouse warmings (Deng et al., 2022). This increase in summer days dominated by weaker meridional pressure gradients has also been reported in previous studies focusing on central Europe (Herrera-Lormendez et al., 2021) and in the prior generation of CMIP GCMs (Otero et al., 2018). The W, NW, SW and the S types, though this last one with a weaker magnitude, show predominant and strong multimodel agreement in their future frequency decrease that extends from the Mediterranean up to the British Isles. This frequency reduction fits the likely increase in MSLP that would directly influence the appearance of this circulation moving further north during the warm season (Ozturk et al., 2021). Nonetheless, the intermodel correlations between the present-day biases and the future frequency changes show high negative values over most of the area where the frequency decrease is projected (Figure S10). Such high correlations further support the statement that projected changes in CT frequencies are sensitive to models' biases in their present-day occurrences. This unexpected result may partly arise from model interdependencies since very similar skills and responses may prevail in some models that share similar atmospheric components. This issue has been observed with models forming statistical dependency groups and might be strongly influenced when evaluated against given reanalysis that result in a priori dependencies (Brands, 2022b).

The remaining CTs displaying significant RF changes are the E and NE configurations. These circulations (E and NE) can advect dry and warm air from the inner continent during their occurrence and are rarely linked to precipitation over western Europe. They exhibit a future increment in frequencies over most of continental Europe. This happens as a response to the less frequent westerly-like circulations. However, despite the good multimodel agreement in the sign of the projected changes in RF of these two CTs (E and NE), a strong disagreement remains in some of the worst performing models over central and western Europe (INM-CM4, INM-CM5 and KACE-1-0-G). These models tend to overestimate the easterly zonal flow frequency with an overall decrease of the intermodel correlation values over these regions (Figure S8).

In general, the CTs have a regional mixed influence on day-to-day summer rainfall over Europe and on its spatial distribution. Their observed frequency changes by the end of the century will result in direct implications for the distribution of precipitation. To this matter, we address the question, to which extent the projected RF changes drive the total precipitation anomalies resulting in the SSP5-8.5 scenario? Figures 6d and S6d show future MMEM summer rainfall changes for each CT. This is determined from the difference of future (F; 2051–2100) minus present (P; 1951–2000) total mean summer rainfall conditioned to the occurrence of a given CT. The more significant changes are found in the C and westerly-like types (W, NW, SW), which are well-known strong modulators of summer precipitation over western Europe. Their projected regional frequency decrease over Europe is mirrored in their future precipitation influence, with dominating negative anomalies (drying).

However, projected changes in precipitation over the European continent do not only arise from frequency changes among the different CTs (between-class, BC effect). The changes within the CTs themselves (within-class, WC effect) can dominate due to changing characteristics of associated weather within the patterns (Cahynová & Huth, 2016; Küttel et al., 2011). To investigate whether the projected frequency changes are the primary reason for the precipitation anomalies, we employ a linear decomposition model from Cattiaux et al. (2013), aiming to decompose the BC versus WC effects as well as Residual (RES) in these changes (Equation (1)). The resultant decomposition for the main five CTs positively contributing to the total seasonal rainfall changes is shown in Figures 6 and S6. The columns from left to right indicate the (a) BC, (b) WC and (c) RES terms and (d) the corresponding SSP5-8.5 projected precipitation changes in each CT resulting from the sum of the three terms (BC + WC + RES).

The first noticeable result is the overall minimal contribution of the RES term to precipitation changes, which will therefore not be further discussed. Key contributions arise from the BC and WC terms. However, the individual contributions do not always add up to the projected change. In many cases, these contributions can regionally

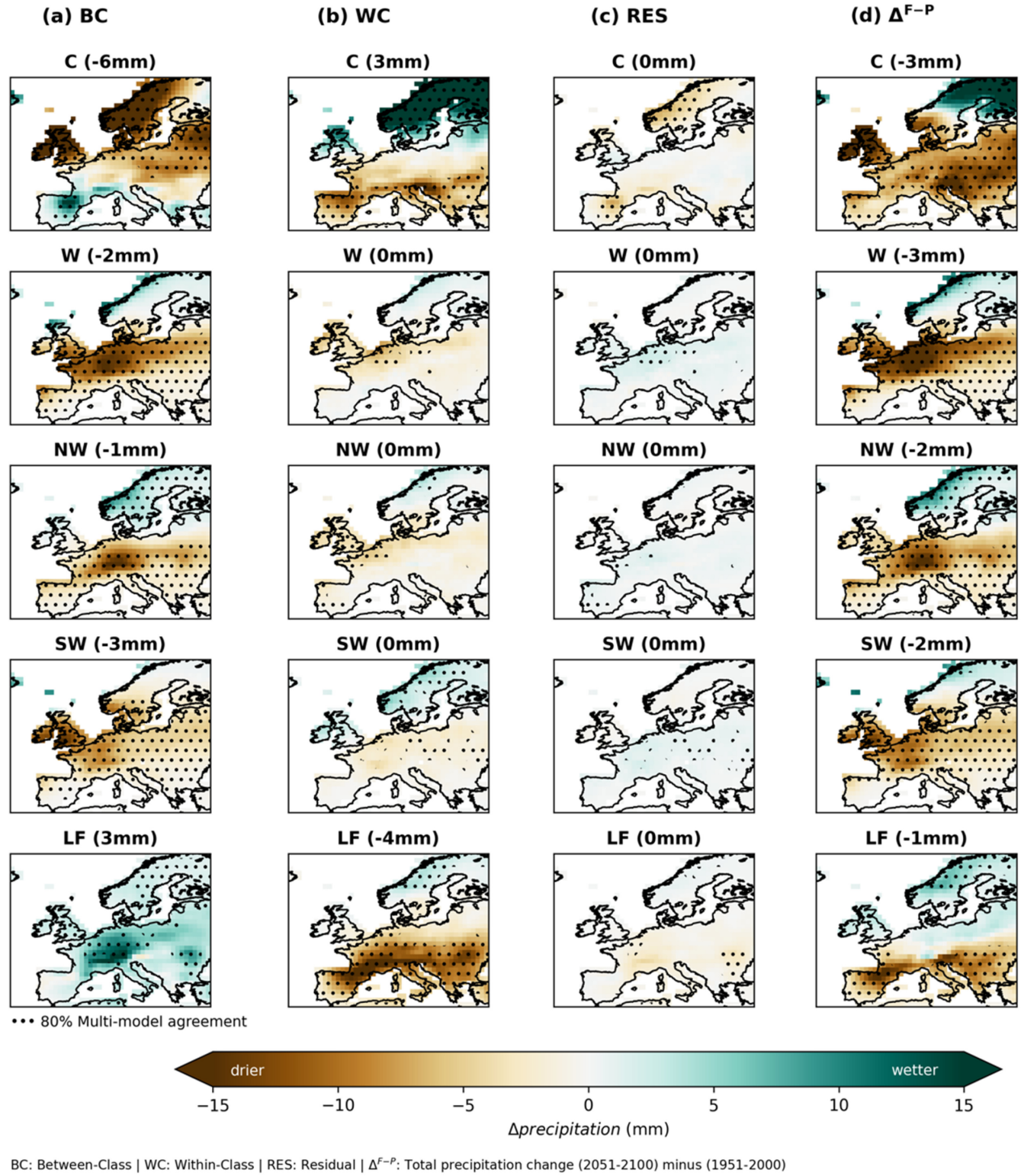

FIGURE 6 Multi-model ensemble mean (MMEM) average decomposition of the summer (JJA) difference in seasonal precipitation corresponding to the five main circulation types, positively contributing to the projected rainfall changes. Precipitation changes are computed using the seasonal difference of the future (F) period 2051–2100 minus the reference period (P) 1951–2000. Stippling indicates 80% sign multimodel agreement. Columns show the (a) BC, (b) WC, (c) RES terms and the (d) absolute future precipitation change $\Delta(F-P)$ obtained from Equation (1), while rows show the CTs. Values in brackets indicate the mean pan-European spatial values. Complementary plots found in Figure S6 [Colour figure can be viewed at wileyonlinelibrary.com]

offset or complement each other. This applies to the cyclonic type, which is the largest positive contributor to the projected total summer precipitation anomalies. The BC term shows that the changes in RF would directly result in drying over northern Europe where cyclonic conditions are expected to decrease in frequency. Consequently, their projected frequency increase over the Mediterranean coasts would lead to some localized wetter conditions. However, the WC term suggest that cyclones would be an important contributor to the drying over the south and towards wetter conditions over the north, advocating that the main contribution to the precipitation changes arises from the WC effect. In many cases, we can see that the BC and WC patterns are somewhat symmetric and partly cancel each other. This means that we cannot only account for CT frequency changes to explain future changes in summer rainfall, but that changes in weather itself, in other words thermodynamical and smaller scale dynamical changes within the CTs might, in some cases, have a stronger final say in some of these projected precipitation anomalies.

Interestingly, for the westerly types, the rainfall changes can almost entirely be attributed to their future expected less frequent influence over Europe (i.e., drier future conditions) as they will shift poleward and become more frequent along the northernmost latitudes of Europe (wetter future conditions). A similar behaviour appears in the other westerly-like CTs, that is, the NW and W types. In both cases, the BC term remains the main contributor to the future rainfall changes due to the weakened occurrence of these circulations over western Europe.

A noticeable behaviour also appears in the LF type. Here, the BC term suggests that an expected future frequency increase in LF conditions would lead to more precipitation, whereas the WC term would imply a projected drying over southern Europe. The relevance of the WC term confirms that frequency changes are not primarily responsible for the observed changes attributable to climate change (Marvel et al., 2019) and projected drying over the Mediterranean-like climates (Seager et al., 2019). This happens as subtropical conditions (weaker pressure gradients) extend their influence poleward, where the CTs dynamics become a less important factor for future changes. Instead, thermodynamical effects and other factors embedded in the WC term will have a stronger influence on the drying over the Mediterranean and extending inland over Europe. Out of the remaining CTs (Figure S6), the observed decomposition can tell us that much of the projected drying over the south will arise from the WC term, where the dynamics of the synoptic patterns play a less important role during summer. Surprisingly, the A type, the most frequent circulation, does not stand out as one of the largest positive contributors to the future precipitation anomalies. It will play a role in the wetter conditions over Scandinavia due to increased moisture transport, but the drying over Europe will be dominated by the nondynamical factors as seen in the WC term. As for the Easterlies, the contributions arising from the BC and WC terms are partly cancelling each other. The future frequency decrease in Easterlies and NE over continental Europe results, according to the BC term, in a general increase of the summer precipitation. But the WC effect suggests a corresponding drying over southern Europe.

The complex individual influence of these circulations can be summarized in Figure 7. Here, we show the summary of the contributions of each CT along each term of the decomposition (BC, WC, RES and $\Delta^{F\text{-}P}$). Overall, the frequency changes of the CTs can explain most of the projected summer drying over the British Isles and partly along the 50° latitude belt. Still, most of the expected changes will result from WC variations. The dominant drivers for within-class variations can arise from (a) smaller-scale phenomena, like orographically forced rain or mesoscale storms (Beck et al., 2007), (b) modification in precipitation-generating processes and/or model inability to accurately simulate these processes (Santos et al., 2016), (c) an increased convective inhibition due to a projected decrease in near-surface relative humidity (Chen et al., 2020; Douville et al., 2020) or (d) from SST influence on horizontal moisture transport (Douville et al., 2020).

When analysing the intermodel correlation of the present-day biases and future precipitation changes for the individual circulation types (Figure S11), the dependencies on model biases are considerably weaker than in the former RF evaluation. Many GCMs, despite showing significant shortcomings in capturing dry days conditioned to the occurrence of CTs, do a good job at reproducing the seasonal total mean precipitation. The observed regional high correlation values between the biases and projected changes result from marked biases that prevail in some individual models like the BCC-CSM2-MR, INM-CM4-8 and INM-CM5-0 (Figures S12 and S13). Thus, the projected JJA precipitation changes conditioned to the synoptic circulations are mostly not strongly influenced by the present-day precipitation biases. Regional high intermodel correlations remain and should be further studied with a larger set of less interdependent GCMs.

4 | SUMMARY AND CONCLUSIONS

We have employed an adapted version of the JCC at each grid cell of a 1° by 1° horizontal grid over Europe (−15°–

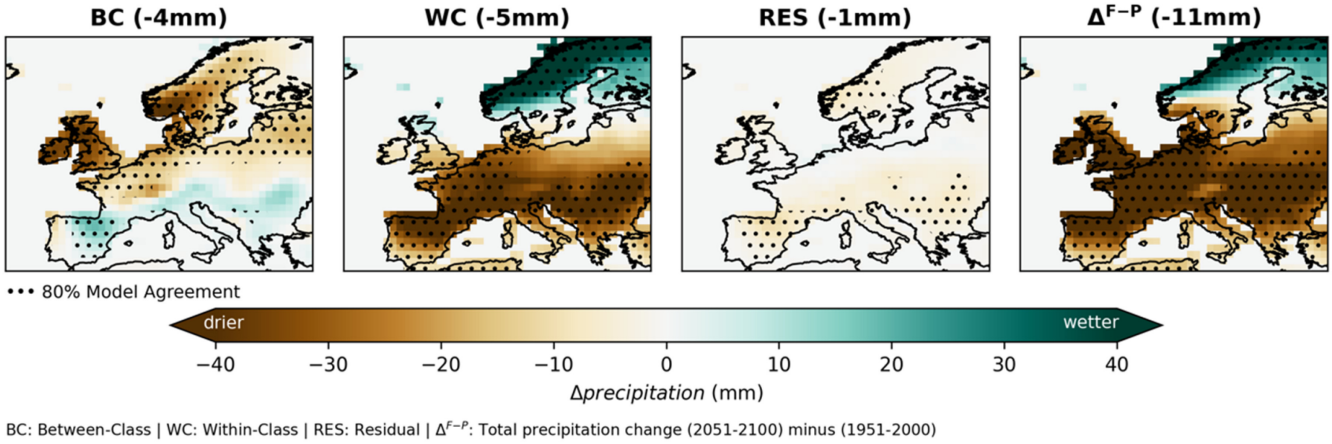

FIGURE 7 Multi-model ensemble mean (MMEM) total decomposition of the summer (JJA) contribution of the 11 circulation types to the difference in seasonal precipitation given Equation (1). Precipitation changes are computed using the seasonal difference of the future (F) period 2051–2100 minus the reference period (P) 1951–2000. Stippling indicates 80% sign multimodel agreement. Values in brackets indicate the mean pan-European spatial values [Colour figure can be viewed at wileyonlinelibrary.com]

30°E and 35°–75°N) to define CTs in summer from daily MSLP fields of the ERA5 reanalyses and of a selection of 21 GCMs from CMIP6. First, we have evaluated the models' ability to reproduce current summer relative frequencies of a reduced set of 11 CTs and to capture the spatial pattern of CPDD as compared to the combined ERA/E-OBS gridded datasets. Our results demonstrate a strong relationship between CTs and dry days at all locations. Anticyclones and easterly-like types (NE, E and SE) are the main synoptic patterns that favour dry days occurrence. In contrast, cyclonic and westerly circulations strongly favour precipitation over western Europe. Climate models are generally good at reproducing the MMEM spatial frequency characteristics of the synoptic types during the summer season. Biases remain in capturing low-flow type frequencies over the Mediterranean. In comparison with CMIP5 (Otero et al., 2018), models continue to underestimate the frequency of the westerly types in the midlatitude belt while overestimating easterly types' during summer. The lowest skills in the individual GCMs are confined to the anticyclonic centres and easterly directions (NE, E, SE), which interestingly are the ones having some of the strongest regional influence on the occurrence of dry days. Moreover, global models do a poor job at reproducing the spatial CDPDD. They tend to overestimate the number of dry days over continental central and southern Europe and specially during the occurrence of the rainy CTs. Over Scandinavia, they generally overestimate the number of wet days in most CTs (except S and SE).

The extended influence of CTs on monthly precipitation was investigated. Summer months with SPI gridded values below −1 (i.e., dry months) were distinguished. The anomalous frequency of the CTs conditional to such dry months was evaluated. A clear regional relationship emerges between CTs responsible for dry days (A and E types); their regional frequency increases during dry months. Overall, the MME approach as well as the individual models (at least 80% multimodel agreement over regions with the largest influences) accurately represents the spatial influence of CTs on dry months when compared to the combined reference ERA5/E-OBS dataset. The more visible positive anomalies appear within the anticyclonic and easterly types. Anticyclones have a more decisive influence over the eastern Europe, whereas the easterlies are more likely to increase in frequency during dry months along western Europe. In response, the rainy CTs (cyclones and westerlies) tend to appear less frequently.

Major changes in seasonal precipitation and dry days have been shown to arise partly from changes in the frequency of the zonal-like CTs, at least in the high-emission scenario SSP5-8.5 selected in our study. The projected decrease in frequency of some of the rainy-like and westerly component synoptic patters (C, W, NW and SW) will play an important role for the projected drying of western Europe. Days dominated by weak pressure gradients (low-flow type) are projected to increase over most of the domain albeit more strongly over the Mediterranean. This increase will enhance the drying projected over southern Europe, likely due to WC contributions, for instance advection of air masses with lower relative humidity due to a land–sea warming contrast (Byrne & O'Gorman, 2013), and to lower relative humidity, associated with a stronger inhibition of deep convection and more dry days (Douville & John, 2021). Part of the remaining projected drying over western and central Europe is strongly driven by WC contributions

arising from anticyclones and from the less frequent easterly and northeasterly types. Whereas the confined wetter conditions over Scandinavia are likely to be driven mainly by the northerly circulations and cyclones. Such changes are congruent with the projected extension of dry and stable summer conditions and the mean poleward shift of moisture corridors and associated atmospheric rivers over Europe (Sousa et al., 2020). However, it remains challenging to interpret the WC contributions as far as the vertical structure of the CTs in not analysed in more details. Further investigation is also needed to better understand the temperature and humidity features of the upstream air masses and their model-dependent sensitivity to climate change.

The investigated projected changes in RF and summer precipitation showed a strong multimodel agreement (80%) in the sign of the projected anomalies. However, the explored intermodel correlation revealed that in some of the cases the projected RF changes are strongly conditioned by present-day biases observed in some of the worst-performing GCMs. This is especially true in the westerly-like CTs, where a large spread prevails in the spatial representation of this flow. Such uncertainties, arising from the present-day biases, appear to not strongly propagate to the projected precipitation changes conditioned to the CTs. Further investigation is recommended with a larger sample of more interdependent GCMs to understand the sources of multimodel disagreement arising from the incorrect spatial representation of some synoptic circulations.

Our study is a snapshot of the main CTs' large-scale characteristics. One might argue that during the summer season, some distinction should be acknowledged in the different types of cyclones that regulate precipitation over the continent. Some of these summer cyclones differentiate themselves from the typical eastward-propagating Atlantic low-pressures, that is, with origins that can be tracked more on the lee side of the Alps which later move northwards (Hofstätter et al., 2016). Here, we do not study the direction of propagation of such circulations which raises the question of whether these "anomalously" propagating cyclones are properly captured as C types or not. Further investigation not only in the changes in frequencies but also in the flow components should be addressed in future analyses.

AUTHOR CONTRIBUTIONS

Pedro Herrera-Lormendez: Investigation; conceptualization; methodology; visualization; writing – original draft; data curation; formal analysis. **Amal John:** Conceptualization; methodology; visualization; writing – review and editing; data curation. **Hervé Douville:** Conceptualization; writing – review and editing; validation; methodology; supervision. **Jörg Matschullat:** Supervision; methodology; validation; writing – review and editing; conceptualization.

ACKNOWLEDGEMENTS

We thankfully acknowledge funding through the EU International Training Network (ITN) Climate Advanced Forecasting of sub-seasonal Extremes (CAFE). The project is supported by the European Union's Horizon 2020 research and innovation programme under the Marie Skłodowska-Curie Grant Agreement No. 813844. We aknowledge the use of the Py-ART python module to create some of the colormaps in the figures. Open Access funding enabled and organized by Projekt DEAL.

DATA AVAILABILITY STATEMENT

The automated gridded JCC has been developed into a Python module. Code and documentation are freely available in https://github.com/PedroLormendez/jcclass.

ORCID

Pedro Herrera-Lormendez https://orcid.org/0000-0003-0982-0032

REFERENCES

Adams, J. (2017) *climate_indices. An open-source python library providing reference implementations of commonly-used climate indices*. Available from: https://github.com/monocongo/climate_indices

Bandhauer, M., Isotta, F., Lakatos, M., Lussana, C., Båserud, L., Izsák, B. et al. (2022) Evaluation of daily precipitation analyses in E-OBS (v19.0e) and ERA5 by comparison to regional high-resolution datasets in European regions. *International Journal of Climatology*, 42(2), 727–747. Available from: https://doi.org/10.1002/joc.7269

Beck, C., Jacobeit, J. & Jones, P.D. (2007) Frequency and within-type variations of large-scale circulation types and their effects on low-frequency climate variability in Central Europe since 1780. *International Journal of Climatology*, 27(4), 473–491. Available from: https://doi.org/10.1002/joc.1410

Belleflamme, A., Fettweis, X. & Erpicum, M. (2015) Do global warming-induced circulation pattern changes affect temperature and precipitation over Europe during summer? *International Journal of Climatology*, 35(7), 1484–1499. Available from: https://doi.org/10.1002/joc.4070

Brands, S. (2022a) A circulation-based performance atlas of the CMIP5 and 6 models for regional climate studies in the Northern Hemisphere mid-to-high latitudes. *Geoscientific Model Development*, 15(4), 1375–1411. Available from: https://doi.org/10.5194/gmd-15-1375-2022

Brands, S. (2022b) Common error patterns in the regional atmospheric circulation simulated by the CMIP multi-model ensemble. *Geophysical Research Letters*, 49, e2022GL101446. Available from: https://doi.org/10.1029/2022GL101446

Burt, T.P. & Ferranti, E.J.S. (2012) Changing patterns of heavy rainfall in upland areas: a case study from northern England. *International Journal of Climatology*, 32(4), 518–532. Available from: https://doi.org/10.1002/JOC.2287

Byrne, M.P. & O'Gorman, P.A. (2013) Land–ocean warming contrast over a wide range of climates: convective quasi-equilibrium theory and idealized simulations. *Journal of Climate*, 26(12), 4000–4016. Available from: https://doi.org/10.1175/JCLI-D-12-00262.1

Cahynová, M. & Huth, R. (2016) Atmospheric circulation influence on climatic trends in Europe: an analysis of circulation type classifications from the COST733 catalogue. *International Journal of Climatology*, 36(7), 2743–2760. Available from: https://doi.org/10.1002/joc.4003

Cattiaux, J., Douville, H., Ribes, A., Chauvin, F. & Plante, C. (2013) Towards a better understanding of changes in wintertime cold extremes over Europe: a pilot study with CNRM and IPSL atmospheric models. *Climate Dynamics*, 40(9–10), 2433–2445. Available from: https://doi.org/10.1007/s00382-012-1436-7

Chen, D. (2000) A monthly circulation climatology for Sweden and its application to a winter temperature case study. *International Journal of Climatology*, 20(10), 1067–1076. Available from: https://doi.org/10.1002/1097-0088(200008)20:10<1067::AID-JOC528>3.0.CO;2-Q

Chen, J., Dai, A., Zhang, Y. & Rasmussen, K.L. (2020) Changes in convective available potential energy and convective inhibition under global warming. *Journal of Climate*, 33(6), 2025–2050. Available from: https://doi.org/10.1175/JCLI-D-19-0461.1

Cornes, R.C., van der Schrier, G., van den Besselaar, E.J.M. & Jones, P.D. (2018) An ensemble version of the E-OBS temperature and precipitation data sets. *Journal of Geophysical Research: Atmospheres*, 123(17), 9391–9409. Available from: https://doi.org/10.1029/2017JD028200

Delaygue, G., Brönnimann, S., Jones, P.D., Blanchet, J. & Schwander, M. (2019) Reconstruction of Lamb weather type series back to the eighteenth century. *Climate Dynamics*, 52(9–10), 6131–6148. Available from: https://doi.org/10.1007/s00382-018-4506-7

Demuzere, M., Werner, M., van Lipzig, N.P.M. & Roeckner, E. (2009) An analysis of present and future ECHAM5 pressure fields using a classification of circulation patterns. *International Journal of Climatology*, 29(12), 1796–1810. Available from: https://doi.org/10.1002/joc.1821

Deng, K., Liu, W., Azorin-Molina, C., Yang, S., Li, H., Zhang, G. et al. (2022) Terrestrial stilling projected to continue in the northern hemisphere mid-latitudes. *Earth's Futures*, 10(7), e2021EF002448. Available from: https://doi.org/10.1029/2021EF002448

Donat, M.G., Leckebusch, G.C., Pinto, J.G. & Ulbrich, U. (2010) European storminess and associated circulation weather types: future changes deduced from a multi-model ensemble of GCM simulations. *Climate Research*, 42(1), 27–43. Available from: https://doi.org/10.3354/cr00853

Douville, H., Decharme, B., Delire, C., Colin, J., Joetzjer, E., Roehrig, R. et al. (2020) Drivers of the enhanced decline of land near-surface relative humidity to abrupt 4xCO_2 in CNRM-CM6-1. *Climate Dynamics*, 55(5–6), 1613–1629. Available from: https://doi.org/10.1007/s00382-020-05351-x

Douville, H. & John, A. (2021) Fast adjustment versus slow SST-mediated response of daily precipitation statistics to abrupt 4xCO_2. *Climate Dynamics*, 56(3–4), 1083–1104. Available from: https://doi.org/10.1007/S00382-020-05522-W

Douville, H., Raghavan, K., Renwick, J., Allan, R.P., Arias, P.A., Barlow, M. et al. (2021) Water cycle changes. In: Masson-Delmotte, V., Zhai, P., Pirani, A., Connors, S.L., Péan, C., Berger, S. et al. (Eds.) *Climate change 2021: the physical science basis. Contribution of working group I to the sixth assessment report of the intergovernmental panel on climate change*. Cambridge and New York, NY: Cambridge University Press, pp. 1055–1210. Available from: https://doi.org/10.1017/9781009157896.010

Edwards, D.C. & McKee, T.B. (1997) *Characteristics of 20th century drought in the United States at multiple time scales*. Fort Collins, CO: Department of Atmospheric Science, Colorado State University. Climatology report: 97-2.

El Kenawy, A.M., McCabe, M.F., Stenchikov, G.L. & Raj, J. (2014) Multi-decadal classification of synoptic weather types, observed trends and links to rainfall characteristics over Saudi Arabia. *Frontiers in Environmental Science*, 2, 37. Available from: https://doi.org/10.3389/fenvs.2014.00037

Eyring, V., Bony, S., Meehl, G.A., Senior, C.A., Stevens, B., Stouffer, R.J. et al. (2016) Overview of the coupled model intercomparison project phase 6 (CMIP6) experimental design and organization. *Geoscientific Model Development*, 9(5), 1937–1958. Available from: https://doi.org/10.5194/gmd-9-1937-2016

Fernández-Granja, J.A., Brands, S., Bedia, J., Casanueva, A. & Fernández, J. (2023) Exploring the limits of the Jenkinson–Collison weather types classification scheme: a global assessment based on various reanalyses. *Climate Dynamics*, 1, 1–17. Available from: https://doi.org/10.21203/RS.3.RS-1415588/V1

Fernandez-Granja, J.A., Casanueva, A., Bedia, J. & Fernandez, J. (2021) Improved atmospheric circulation over Europe by the new generation of CMIP6 earth system models. *Climate Dynamics*, 56, 3527–3540. Available from: https://doi.org/10.1007/s00382-021-05652-9

Grise, K.M. & Davis, S.M. (2020) Hadley cell expansion in CMIP6 models. *Atmospheric Chemistry and Physics*, 20(9), 5249–5268. Available from: https://doi.org/10.5194/acp-20-5249-2020

Herrera-Lormendez, P. (2022) PedroLormendez/jcclass:v0.0.2 (v0.0.2). *Zenodo*. https://doi.org/10.5281/zenodo.7057289

Herrera-Lormendez, P., Mastrantonas, N., Douville, H., Hoy, A. & Matschullat, J. (2021) Synoptic circulation changes over central Europe from 1900 to 2100—Reanalyses and CMIP6. *International Journal of Climatology.*, 42, 4062–4077. Available from: https://doi.org/10.1002/joc.7481

Hersbach, H., Bell, B., Berrisford, P., Hirahara, S., Horányi, A., Muñoz-Sabater, J. et al. (2020) The ERA5 global reanalysis. *Quarterly Journal of the Royal Meteorological Society*, 146(730), 1999–2049. Available from: https://doi.org/10.1002/qj.3803

Hofstätter, M., Chimani, B., Lexer, A. & Blöschl, G. (2016) A new classification scheme of European cyclone tracks with relevance to precipitation. *Water Resources Research*, 52(9), 7086–7104. Available from: https://doi.org/10.1002/2016WR019146

Hoy, A., Schucknecht, A., Sepp, M. & Matschullat, J. (2014) Large-scale synoptic types and their impact on European precipitation. *Theoretical and Applied Climatology*, 116(1–2), 19–35. Available from: https://doi.org/10.1007/s00704-013-0897-x

Huguenin, M.F., Fischer, E.M., Kotlarski, S., Scherrer, S.C., Schwierz, C. & Knutti, R. (2020) Lack of change in the projected frequency and persistence of atmospheric circulation types over central Europe. *Geophysical Research Letters*, 47(9),

e2019GL086132. Available from: https://doi.org/10.1029/2019GL086132

Huth, R., Beck, C., Philipp, A., Demuzere, M., Ustrnul, Z., Cahynová, M. et al. (2008) Classifications of atmospheric circulation patterns. *Annals of the New York Academy of Sciences*, 1146(1), 105–152. Available from: https://doi.org/10.1196/annals.1446.019

Ionita, M., Nagavciuc, V., Kumar, R. & Rakovec, O. (2020) On the curious case of the recent decade, mid-spring precipitation deficit in central Europe. *npj Climate and Atmospheric Science*, 3(1), 1–10. Available from: https://doi.org/10.1038/s41612-020-00153-8

Jenkinson, A.F. & Collison, F.P. (1977) *An initial climatology of gales over the North Sea*. Bracknell: Meteorological Office. Synoptic climatology branch memorandum: 62.

Jones, P.D., Harpham, C. & Lister, D. (2016) Long-term trends in gale days and storminess for The Falkland Islands. *International Journal of Climatology*, 36(3), 1413–1427. Available from: https://doi.org/10.1002/joc.4434

Jones, P.D., Hulme, M. & Briffa, K.R. (1993) A comparison of Lamb circulation types with an objective classification scheme. *International Journal of Climatology*, 13(6), 655–663. Available from: https://doi.org/10.1002/joc.3370130606

Kautz, L.-A., Martius, O., Pfahl, S., Pinto, J.G., Ramos, A.M., Sousa, P.M. et al. (2022) Atmospheric blocking and weather extremes over the Euro-Atlantic sector—a review. *Weather and Climate Dynamics*, 3(1), 305–336. Available from: https://doi.org/10.5194/wcd-3-305-2022

Küttel, M., Luterbacher, J. & Wanner, H. (2011) Multidecadal changes in winter circulation-climate relationship in Europe: frequency variations, within-type modifications, and long-term trends. *Climate Dynamics*, 36(5–6), 957–972. Available from: https://doi.org/10.1007/s00382-009-0737-y

Lamb, H.H. (1972) *British Isles weather types and a register of daily sequence of circulation patterns, 1861–1971: geophysical memoir*. London: HMSO.

Lhotka, O., Trnka, M., Kyselý, J., Markonis, Y., Balek, J. & Možný, M. (2020) Atmospheric circulation as a factor contributing to increasing drought severity in Central Europe. *Journal of Geophysical Research: Atmospheres*, 125(18), e2019JD032269. Available from: https://doi.org/10.1029/2019JD032269

Lorenzo, M.N., Ramos, A.M., Taboada, J.J. & Gimeno, L. (2011) Changes in present and future circulation types frequency in northwest Iberian Peninsula. *PLoS One*, 6(1), e16201. Available from: https://doi.org/10.1371/journal.pone.0016201

Marvel, K., Cook, B.I., Bonfils, C.J.W., Durack, P.J., Smerdon, J.E. & Williams, A.P. (2019) Twentieth-century hydroclimate changes consistent with human influence. *Nature*, 569(7754), 59–65. Available from: https://doi.org/10.1038/s41586-019-1149-8

Mastrantonas, N., Magnusson, L., Pappenberger, F. & Matschullat, J. (2022) What do large-scale patterns teach us about extreme precipitation over the Mediterranean at medium- and extended-range forecasts? *Quarterly Journal of the Royal Meteorological Society*, 148, 875–890. Available from: https://doi.org/10.1002/QJ.4236

McKee, T.B., Doesken, N.J. & Kleist, J. (1993) The relationship of drought frequency and duration to time scale. In: *Proceedings of the eight conference on applied climatology*. Anaheim: American Meteorological Society, pp. 179–184.

Neal, R., Fereday, D., Crocker, R. & Comer, R.E. (2016) A flexible approach to defining weather patterns and their application in weather forecasting over Europe. *Meteorological Applications*, 23, 389–400. Available from: https://doi.org/10.1002/met.1563

Otero, N., Sillmann, J. & Butler, T. (2018) Assessment of an extended version of the Jenkinson–Collison classification on CMIP5 models over Europe. *Climate Dynamics*, 50(5–6), 1559–1579. Available from: https://doi.org/10.1007/s00382-017-3705-y

Oudar, T., Cattiaux, J. & Douville, H. (2020) Drivers of the northern extratropical eddy-driven jet change in CMIP5 and CMIP6 models. *Geophysical Research Letters*, 47(8), e2019GL086695. Available from: https://doi.org/10.1029/2019GL086695

Ozturk, T., Matte, D. & Christensen, J.H. (2021) Robustness of future atmospheric circulation changes over the EURO-CORDEX domain. *Climate Dynamics*, 1, 1–16. Available from: https://doi.org/10.1007/S00382-021-06069-0/FIGURES/17

Pfahl, S. (2014) Characterising the relationship between weather extremes in Europe and synoptic circulation features. *Natural Hazards and Earth System Sciences*, 14, 1461–1475. Available from: https://doi.org/10.5194/nhess-14-1461-2014

Phillips, I.D. & McGregor, G.R. (1998) The utility of a drought index for assessing the drought hazard in Devon and Cornwall, South West England. *Meteorological Applications*, 5(4), 359–372. Available from: https://doi.org/10.1017/S1350482798000899

Priestley, M.D.K. & Catto, J.L. (2022) Future changes in the extratropical storm tracks and cyclone intensity, wind speed, and structure. *Weather and Climate Dynamics*, 3(1), 337–360. Available from: https://doi.org/10.5194/wcd-3-337-2022

Richardson, D., Fowler, H.J., Kilsby, C.G. & Neal, R. (2018) A new precipitation and drought climatology based on weather patterns. *International Journal of Climatology*, 38(2), 630–648. Available from: https://doi.org/10.1002/joc.5199

Santos, J.A., Belo-Pereira, M., Fraga, H. & Pinto, J.G. (2016) Understanding climate change projections for precipitation over western Europe with a weather typing approach. *Journal of Geophysical Research*, 121(3), 1170–1189. Available from: https://doi.org/10.1002/2015JD024399

Sarricolea Espinoza, P., Meseguer-Ruiz, Ó., Martín-Vide, J. & Martín-Vide, J. (2014) Variabilidad y tendencias climáticas en Chile central en el período 1950–2010 mediante la determinación de los tipos sinópticos de Jenkinson y Collison. *Boletín de la Asociación de Geógrafos Españoles*, 64, 227–247. Available from: https://doi.org/10.21138/bage.1688

Schoetter, R., Cattiaux, J. & Douville, H. (2015) Changes of western European heat wave characteristics projected by the CMIP5 ensemble. *Climate Dynamics*, 45(5–6), 1601–1616. Available from: https://doi.org/10.1007/s00382-014-2434-8

Schwarzak, S., Hänsel, S. & Matschullat, J. (2015) Projected changes in extreme precipitation characteristics for central eastern Germany (21st century, model-based analysis). *International Journal of Climatology*, 35(10), 2724–2734. Available from: https://doi.org/10.1002/joc.4166

Seager, R., Osborn, T.J., Kushnir, Y., Simpson, I.R., Nakamura, J. & Liu, H. (2019) Climate variability and change of Mediterranean-type climates. *Journal of Climate*, 32(10), 2887–2915. Available from: https://doi.org/10.1175/JCLI-D-18-0472.1

Shepherd, T.G. (2014) Atmospheric circulation as a source of uncertainty in climate change projections. *Nature Geoscience*, 7(10), 703–708. Available from: https://doi.org/10.1038/NGEO2253

Shepherd, T.G., Boyd, E., Calel, R.A., Chapman, S.C., Dessai, S., Dima-West, I.M. et al. (2018) Storylines: an alternative approach to representing uncertainty in physical aspects of climate change. *Climatic Change*, 151(3–4), 555–571. Available from: https://doi.org/10.1007/S10584-018-2317-9

Sousa, P.M., Ramos, A.M., Raible, C.C., Messmer, M., Tomé, R., Pinto, J.G. et al. (2020) North Atlantic integrated water vapor transport—from 850 to 2100 CE: impacts on western European rainfall. *Journal of Climate*, 33(1), 263–279. Available from: https://doi.org/10.1175/JCLI-D-19-0348.1

Stryhal, J. & Huth, R. (2019a) Classifications of winter atmospheric circulation patterns: validation of CMIP5 GCMs over Europe and the North Atlantic. *Climate Dynamics*, 52(5–6), 3575–3598. Available from: https://doi.org/10.1007/s00382-018-4344-7

Stryhal, J. & Huth, R. (2019b) Trends in winter circulation over the British Isles and central Europe in twenty-first century projections by 25 CMIP5 GCMs. *Climate Dynamics*, 52(1–2), 1063–1075. Available from: https://doi.org/10.1007/s00382-018-4178-3

Svoboda, M., Hayes, M., Wood, D.A. & World Meteorological Organization (WMO). (2012) *Standardized precipitation index user guide*. Geneva: WMO. WMO-No. 1090. Available from: http://library.wmo.int/opac/index.php?lvl=notice_display&id=13682

Trigo, R.M. & DaCamara, C.C. (2000) Circulation weather types and their influence on the precipitation regime in Portugal. *International Journal of Climatology*, 20(13), 1559–1581. Available from: https://doi.org/10.1002/1097-0088(20001115)20:13<1559::AID-JOC555>3.0.CO;2-5

Wilby, R.L., O'Hare, G. & Barnsley, N. (1997) The North Atlantic oscillation and British Isles climate variability, 1865–1996. *Weather*, 52(9), 266–276. Available from: https://doi.org/10.1002/j.1477-8696.1997.tb06323.x

SUPPORTING INFORMATION

Additional supporting information can be found online in the Supporting Information section at the end of this article.

How to cite this article: Herrera-Lormendez, P., John, A., Douville, H., & Matschullat, J. (2023). Projected changes in synoptic circulations over Europe and their implications for summer precipitation: A CMIP6 perspective. *International Journal of Climatology*, *43*(7), 3373–3390. https://doi.org/10.1002/joc.8033